Enzymatic activities of the human AGPAT isoform 3 and isoform 5: localization of AGPAT5 to mitochondria[s]

Sneha S. Prasad, Abhimanyu Garg, and Anil K. Agarwal[1]

Division of Nutrition and Metabolic Diseases, Department of Internal Medicine and Center for Human Nutrition, University of Texas Southwestern Medical Center, Dallas, TX

Abstract The enzyme 1-acylglycerol-3-phosphate-O-acyltransferase (AGPAT) converts lysophosphatidic acid (LPA) to phosphatidic acid (PA). In this study, we show enzymatic properties, tissue distribution, and subcellular localization of human AGPAT3 and AGPAT5. In cells overexpressing these isoforms, the proteins were detected in the nuclear envelope and the endoplasmic reticulum. AGPAT5-GFP fusion protein was localized in the mitochondria of both Chinese hamster ovary and human epithelial cervical cancer cells. Using lysates of AD293 cells infected with AGPAT3 and AGPAT5 recombinant adenovirus, we show that AGPAT3 and AGPAT5 proteins have AGPAT activity. Both the isoforms have similar apparent V_{max} of 6.35 and 2.42 nmol/min/mg protein, respectively, for similar LPA. The difference between the two isoforms is in their use of additional lysophospholipids. AGPAT3 shows significant esterification of lysophosphatidylinositol (LPI) in the presence of C20:4 fatty acid, whereas AGPAT5 demonstrates significant acyltransferase activity toward lysophosphatidylethanolamine (LPE) in the presence of C18:1 fatty acid. The *AGPAT3* mRNA is ubiquitously expressed in human tissues with several-fold differences in the expression pattern compared with the closely related *AGPAT4*.[SB] In summary, we show that in the presence of different fatty acids, AGPAT3 and AGPAT5 prefer different lysophospholipids as acyl acceptors. More importantly, localization of overexpressed AGPAT5 (this study) as well as GPAT1 and 2 (previous studies) in mitochondria supports the idea that the mitochondria might be capable of synthesizing some of their own glycerophospholipids.—Prasad, S. S., A. Garg, and A. K. Agarwal. Enzymatic activities of the human AGPAT isoform 3 and isoform 5: localization of AGPAT5 to mitochondria. *J. Lipid Res.* 2011. 52: 451–462.

Supplementary key words 1-acylglycerol-3-phosphate-O-acyltransferase • LPAAT • acyltransferase • phospholipid • lipodystrophy

Phosphatidic acid (PA) is the main precursor for the synthesis of various downstream glycerophospholipids such as phosphatidyl-serine (PS), -ethanolamine (PE), -choline (PC), and -inositol (PI) (1). PC, PS, and PE are the main phospholipids found in the various cellular membranes, while PI is an important lipid signaling molecule. PA is both a signaling phospholipid and a precursor for the synthesis of triacylglycerol (TAG). The biosynthesis of TAG in eukaryotic cells initiates with the successive esterification of the hydroxyl groups with various fatty acids on the glycerol-3-phosphate backbone (2–4). These acylations are an enzymatic process catalyzed sequentially by glycerol-3-phosphate acyltransferases (GPAT), 1-acylglycerol-3-phosphate-O-acyltransferases (AGPAT), and diacylglycerol acyltransferases (DGAT) enzymes.

PA itself is the product of the acylation of lysophosphatidic acid (LPA), catalyzed by the enzyme AGPAT at the *sn-2* position of the glycerol backbone. Several isoforms of AGPAT are now known, each encoded by a different gene (5–13); however, the biological role of only a few isoforms is known at this time. We had previously shown that mutations in AGPAT2 result in congenital generalized lipodystrophy (CGL), type 1, characterized by near total lack of adipose tissue (AT) from birth (14). Patients with CGL are predisposed

to developing hepatic steatosis, hyperinsulinemia, hyper-triglyceridemia, and diabetes (2). This observation in humans has also been duplicated by targeted gene deletion in mice (15). Another enzyme, referred to as comparative genome identification 58/alpha/beta hydrolase domain 5 (CGI-58/ABHD5), has, in addition to lipid hydrolase activity (16), the signature motif NHX_4D found in all AGPATs (17) and was recently shown to possess AGPAT enzymatic activity (16). Mutations in the CGI-58/ABHD5 gene in humans or targeted gene deletion in mice also results in hepatic steatosis and hepatomegaly but not in lipodystrophy (16). This phenotype in humans is known as Chanarin-Dorfman syndrome (neutral lipid storage disorder) (18). It is interesting to note that CGI-58/ABHD5 lacks a conserved serine residue in the catalytic triad GXSXG that is important for the lipase activity (16). Thus, recombinant CGI-58/ABHD5 lacks lipase activity. Furthermore, its lipase activity is only observed in the presence of adipose triglyceride lipase (ATGL, also known as desnutrin), indicating its role as a coactivator of ATGL. Nevertheless, mutations in CGI-58/ABHD5 result in the loss of lipase activity, resulting in an excessive accumulation of TAG in basal keratinocytes, hepatocytes, myocytes, and leukocytes. A limited understanding of the role of AGPAT6/GPAT4 became available from the $Agpat6^{-/-}$ mice, which displayed reduced subdermal adipose tissue (8, 19). However, AGPAT6 has been reported to display GPAT activity instead of AGPAT activity (AGPAT6/GPAT4) (20, 21). In addition, Janus-faced enzymes Tgl3p and Tgl5p in yeast recently have been reported to have dual lipase and AGPAT enzymatic activities (22). The enzymatic activities are independent of each other. These clinical observations in humans related to the AGPAT2 and CGI-58/ABHD5 encouraged us to further explore the physiology of other AGPAT isoforms.

We have characterized and reported both enzymatic properties and tissue expression for the AGPAT isoforms 8-11 (10–13). These AGPAT isoforms have also been reported to have additional enzymatic activity. AGPAT8 shows acyl-CoA:lysocardiolipin acyltransferase (ALCAT1) activity (23), AGPAT9 shows lysophosphatidylcholine acyltransferase (LPCAT1) activity (24, 25), AGPAT10 shows GPAT3 activity (26), and AGPAT11 shows LPCAT2/lyso platelet activating factor acetyltransferase (Lyso-PAF-AT) activity (27, 28). The GenBank accession number and enzymatic activity of various AGPATs are provided in supplementary Table I. The enzymatic activities of AGPAT1 and AGPAT2 have been described (5, 7). Multiple amino acid sequence alignment of known human AGPATs revealed that AGPAT3 and AGPAT4 are closely related, whereas human AGPAT5 is a singleton. In this study, we chose to investigate AGPAT3 and AGPAT5 and present detailed enzymatic activities for both of the isoforms. Previously, two independent studies have been conducted with mouse AGPAT3, one showing its presence in Golgi apparatus and its possible functions (29), and another demonstrating its enzymatic activity (30). In this study, we present detailed substrate specificities, subcellular localization, and tissue expression for human AGPAT3 and AGPAT5.

METHODS

Generation of V5-epitope-tagged wild-type AGPAT3 and AGPAT5 recombinant adenovirus

We have previously described the generation of recombinant adenovirus using the AdEasy adenoviral system (Stratagene, La Jolla, CA) in detail (12). In brief, the full length open reading frame (OFR) for AGPAT3 and AGPAT5 cDNAs, GenBank accession number NM_020132 and NM_018361, respectively, were tagged with V5-epitope at the amino-terminus by amplifying the cDNA from a plasmid containing the ORF for AGPAT3 and AGPAT5. (The details for the generation of the cDNA for human AGPAT3 and AGPAT5 are described in the supplementary data provided with this article.) AGPAT3 was amplified with primers 5′-CCGCTCGAGATG<u>GGGTAAGCCTATCCCTAACCCTCTCCTCGGTCTCGATTCTACG</u>GGCCTGCTGGCCTTCCTGAAG-3′ and 5′-CCCAAGCTTTTATTCCTTTTTCTTAAAC-3′. Similarly, AGPAT5 was amplified with primers 5′-CCGCTCGAGATG<u>GGGTAAGCCTATCCCTAACCCTCTCCTCGGTCTCGATTCTACG</u>GACGCTGCTGTCCCTGGTGCTCCACACG-3′ and 5′-CCCAAGCTTCTATGCTTTAATAGTAACCC-3′. (The V5 epitope is underlined.) The amplified product was cloned in TA-cloning vector, sequenced, restriction digested with *XhoI* and *HindIII,* and cloned into the pShuttle-CMV vector at the same restriction sites. The orientation of the insert was reconfirmed by restriction digest and sequencing of the plasmid. To generate recombinant adenovirus, the pShuttle-CMV-AGPAT3 and pShuttle-CMV-AGPAT5 plasmids were digested with *PmeI* and cotransformed with pAdEasy-1 into BJ5183 cells. The recombinant AdEasy-1-AGPAT3 and AdEasy-1-AGPAT5 plasmids were digested with *PacI* and transfected in AD293 cells using Lipofectamine-2000 (Invitrogen). Viral pools were further propagated in the same AD293 cells. The viral pool which showed most enzymatic activity was selected for further amplification and purification using the Virabind adenovirus purification kit (Cell Biolabs Inc., San Diego, CA). The generation of recombinant adenovirus-β-galactosidase (LacZ) has been described previously (12).

Generation of EGFP-tagged wild-type AGPAT3 and AGPAT5 expression vector

The construction of the wild-type AGPAT3-GFP fusion protein was carried out using the AGPAT3 cloned in TA cloning vector. The ORF for AGPAT3 was amplified using wild-type plasmid as the template and primer pairs 5′-CCGCTCGAGATGGGGCCTGCTGG-3′ and 5′-CCGGAATTCTTCCTTTTTCTTAAAC-3′. The amplified product and the plasmid pEGFP-N3 (Clontech, Mountain View, CA) were restricted with *XhoI* and *EcoRI* and cloned in the similar sites. The expression plasmid was sequenced to ascertain the orientation and correctness for the junction sequences. The strategy for generating the wild-type AGPAT5-GFP fusion protein was the same, except it was amplified with primer pairs 5′-CCGCTCGAGATGCTGCTGTCCCTG-3′ and 5′-CCGGAATTCTGCTTTAATAGTAAC-3′ and the wild-type plasmid carrying the AGPAT5 sequences.

Processing of the cellular lysates for the enzymatic activity

The enzymatic assays were performed using adenovirally expressed recombinant protein. The AD293 cells were infected with AGPAT3 or AGPAT5 recombinant adenovirus at a multiplicity of infection (MOI) of 100. Note that the method employed for the virus purification yielded a low level of infectious viral particles. After 48 h, the infected cells were collected in the lysis buffer (100 mM Tris pH 7.4, 10 mM NaCl containing protease inhibitor cocktail; Roche, Indianapolis, IN). The cells were lysed

in two different ways: either with three freeze-thaw cycles or via sonication, which was carried out at 65% output (which generates energy of 20 Joules) for three 6 s bursts with intermittent cooling on ice (Sonics Vibra Cell, Newtown, CT). The cell lysate was centrifuged at 3,000 g for 10 min at 4°C to remove the cell debris. Since sonication retained 4-6-fold more AGPAT activity than the freeze-thaw protocol, all the enzymatic activity assays were performed by sonication of frozen lysates (data not shown). The mitochondrial fraction was obtained by centrifuging the supernatant at 13,000 g for 30 min at 4°C. The mitochondrial pellet was washed in the same buffer and used for enzymatic assays. Protein concentration was determined by a commercially available colorimetric assay (Bio-Rad Laboratories, Hercules, CA).

AGPAT enzymatic activity of AGPAT3 and AGPAT5 in the cell lysate

The enzyme activity was determined by measuring the conversion of [³H]LPA to [³H]PA as described previously (12, 31). Briefly, the enzymatic reaction was assembled in 200 μl of 100 mM Tris-HCl buffer pH 7.4 or pH 6.5 for AGPAT3 and AGPAT5, respectively, containing the following: 10 μmol/l LPA (oleoyl-$sn1$-glycerol-3-phosphate; Avanti Polar Lipids, Alabaster, AL); 50 μmol/l oleoyl CoA (Sigma, St. Louis, MO); 1 μl of [³H] oleoyl-LPA (specific activity 30-60 Ci/mmol; PerkinElmer Life and Analytic Sciences, Boston, MA); and 1 mg/ml fatty acid free BSA. The reaction was started by adding 100 μg of cell lysate followed by incubation for 10 min at 37°C for AGPAT3 and at 30°C for AGPAT5. The reaction was terminated by adding 0.5 ml of 1-butanol containing 1N-HCl and unlabeled LPA and PA to extract phospholipids. The butanol extract was dried under vacuum, and the LPA and PA were resolved using the solvent system chloroform-methanol-acetic acid-water (25:10:3:1). Radioactive spots were identified by comigration with unlabeled LPA and PA standard and visualized in iodine vapors. The [³H]LPA and [³H]PA spots were scraped and counted for radioactivity (Tri-Carb Liquid Scintillation Counter 3100TR; PerkinElmer Life Sciences, Boston, MA).

Determination of the acyltransferase activity for additional lysophospholipids (LPE, LPC, LPG, LPI and LPS) containing the C18:1 fatty acid at the *sn-1* position was determined as above, except the lysophospholipids were substituted for LPA.

Acyl-CoA specificity

The specificity of esterification of *sn*-2 position of [³H]LPA (*sn*-1-oleoyl-2-hydroxy-*sn*-glycerol-3-phosphate) was determined by using the following acyl-CoAs: octanoyl (C8:0)-, decanoyl (C10:0)-, lauroyl (C12:0)-, tridecanoyl (C13:0)-, myristoyl (C14:0)-, pentadecanoyl (C15:0)-, palmitoyl (C16:0)-, heptadecanoyl (C17:0)-, stearoyl (C18:0)-, oleoyl (C18:1)-, linoleoyl (C18:2)-, linolenoyl (C18:3;n-3)-, γ-linolenoyl (C18:3;n-6)-, nonadecanoyl (C19:0)-, arachidoyl (C20:0)-, arachidonoyl (C20:4;n-6)-, heneicosanoyl (C21:0)-, behenoyl (C22:0)-, docosahexaenoyl (C22:6;n-3)-, tricosanoyl (C23:0)-, ligneceroyl (C24:0)-, nervonoyl (C24:1;n-9)-, pentacosanoyl (C25:0)-, and hexacosanoyl (C26:0)-CoA. The assay conditions remained the same as described for the AGPAT activity.

sn-1-acyl-lysophaditic acid specificity

To determine the specificity of various LPAs for the enzymatic activity, the following LPAs with various fatty acids at *sn*-1 position were used for the assay: palmitoyl (C16:0)-, heptadecanoyl (C17:0)-, stearoyl (C18:0)-, arachidonoyl (C20:4)-, and oleoyl (C18:1)-CoA. The enzymatic assay was assembled as before, except unlabeled LPAs and [¹⁴C]oleoyl-CoA were used as substrates, and the activity was determined by formation of [¹⁴C]PA. In a separate experiment, we resolved various species of LPA and PA in the same solvent system and found no difference in their mobility on the thin layer chromatography plate (supplementary Fig. I).

Western blot analysis

HEK-293 cells overexpressing V5 tagged AGPAT3 and AGPAT5 were collected and lysed in RIPA buffer containing protease inhibitor cocktail (Roche, Indianapolis, IN). Lysates were centrifuged at 3,000 g for 10 min at 4°C to remove cellular debris (whole-cell lysate, WCL). The post 3,000 g supernatant was subjected to differential centrifugation to obtain fractions containing mitochondria or microsomes. Protein concentrations were determined using Bio-Rad DC protein assay (BioRad, Hercules, CA). Total protein (30 μg) from WCL was resolved on 10% SDS-PAGE, followed by transfer onto nylon membrane (Millipore, Billerica, MA). The membrane was blocked with 5% nonfat milk containing 0.2% Tween-20 and then incubated with V5 antibody (dilution 1:5000) conjugated to horseradish alkaline phosphatase

TABLE 1. ΔCt values for human *AGPAT3-5* in tissues and fold changes among isoforms

Tissue	AGPAT3[a]	AGPAT4[a]	AGPAT5[a]	AGPAT3 versus AGPAT4[b]	AGPAT3 versus AGPAT5[b]	AGPAT4 versus AGPAT5[b]
Heart	6.98	11.56	12.94	23.92	62.25	2.60
Brain	7.03	7.18	9.47	1.11	5.43	4.89
Placenta	6.54	8.3	8.14	3.39	3.03	0.90
Skeletal muscle	9.66	14.92	14.45	38.32	27.67	0.72
Kidney	4.74	9.82	10.85	33.82	69.07	2.04
Pancreas	4.4	8.15	8.37	13.45	15.67	1.16
Lung	5.43	8.27	9.55	7.16	17.39	2.43
Spleen	6.2	7.79	9.62	3.01	10.70	3.56
Thymus	7.74	10.08	10.05	5.06	4.96	0.98
Prostate	7.56	10.29	7.1	6.63	0.73	0.11
Testis	3.9	7.94	5.32	16.45	2.68	0.16
Ovary	8.23	8.31	10.75	1.06	5.74	5.43
Small intestine	8.5	8.62	10.91	1.09	5.31	4.89
Colon	7.44	9.51	9.58	4.20	4.41	1.05
Leukocyte	5.92	7.33	11.52	2.66	48.50	18.25
Adipose	6.03	7.48	10.08	2.73	16.56	6.06
Liver	5.49	10.95	9.57	44.02	16.91	0.38

The ΔCt values as quantified by TaqMan real time PCR. Shown are the mean ΔCt values, performed in duplicate and normalized for internal control *G3PDH*. Fold increase between isoforms in various tissues were calculated $2^{-\Delta\text{Ct}}$ according to Ref. 37. Data for human AGPAT5 are from Ref. 10. AGPAT, 1-acylglycerol-3-phosphate-O-acyltransferase.

[a] The lower the ΔCt value, the higher the expression in the tissue.

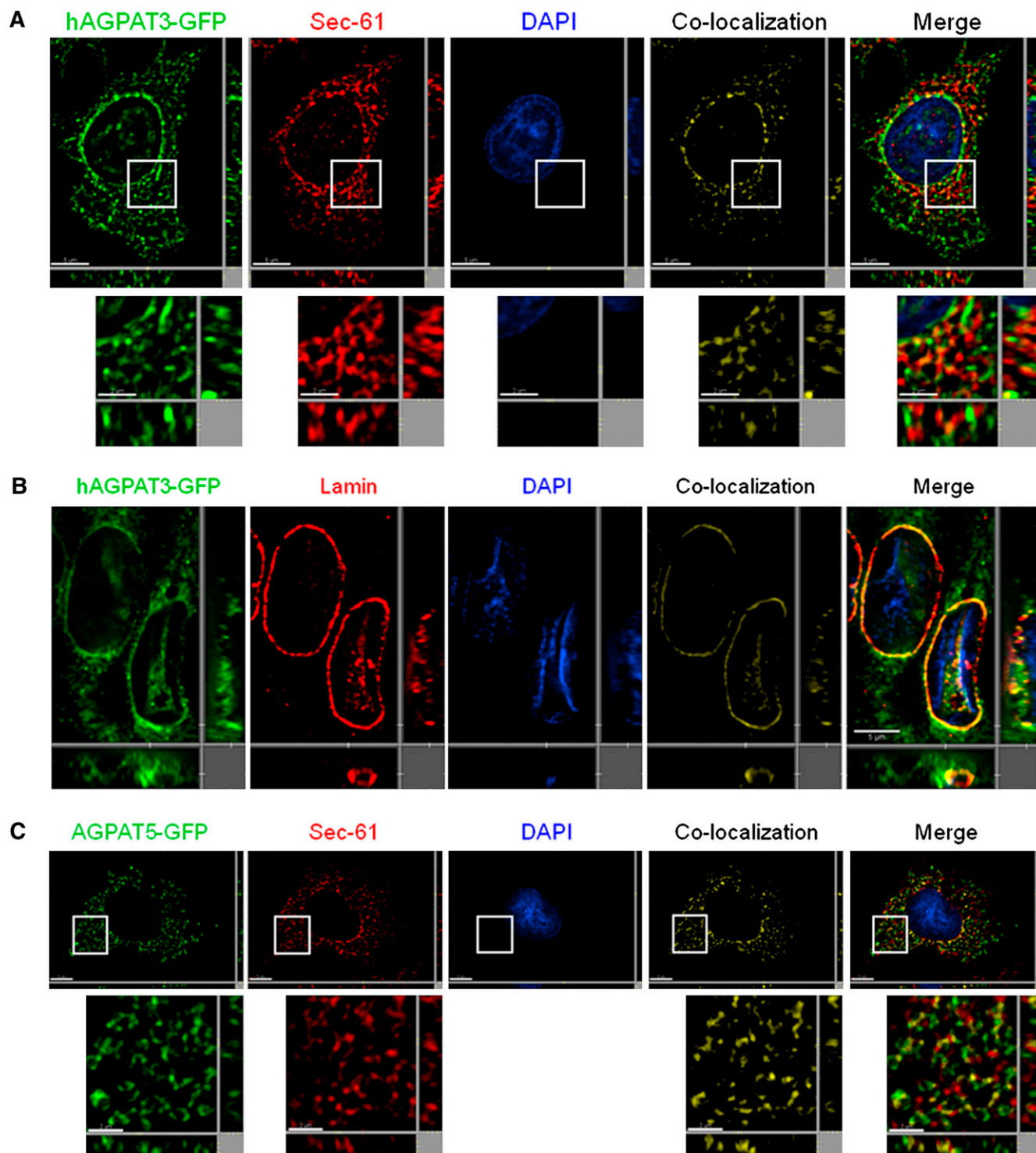[b] Values are fold changes between isoforms.

Fig. 1. Localization of AGPAT3-GFP and AGPAT5-GFP to endo-membranes in cultured cells. A, B: CHO cells overexpressing AGPAT3-GFP were fixed in methanol and incubated with antibody sec61β specific for endoplasmic reticulum and lamin A/C specific for nuclear lamina and imaged for green and red fluorescence using fluorescence microscopy. Shown are representative images for AGPAT3 (green fluorescence), sec61β (red fluorescence), DAPI (blue fluorescence), colocalization channel (yellow fluorescence), and the merged image. C, D: Fluorescence images for AGPAT5-GFP expressed in CHO cells. Cells for sec61β and lamin A/C were processed as above. E: The AGPAT5-GFP expressing cells were incubated with MitoTracker Red dye, fixed in 4% paraformaldehyde, and imaged as before. Shown for each image is a single z-stack image, where the x and y axes show the z-stacks. Scale bar: 5 μm for larger images and 2 μm for higher magnification images. AGPAT, 1-acylglycerol-3-phosphate-O-acyltransferase; CHO, Chinese hamster ovary.
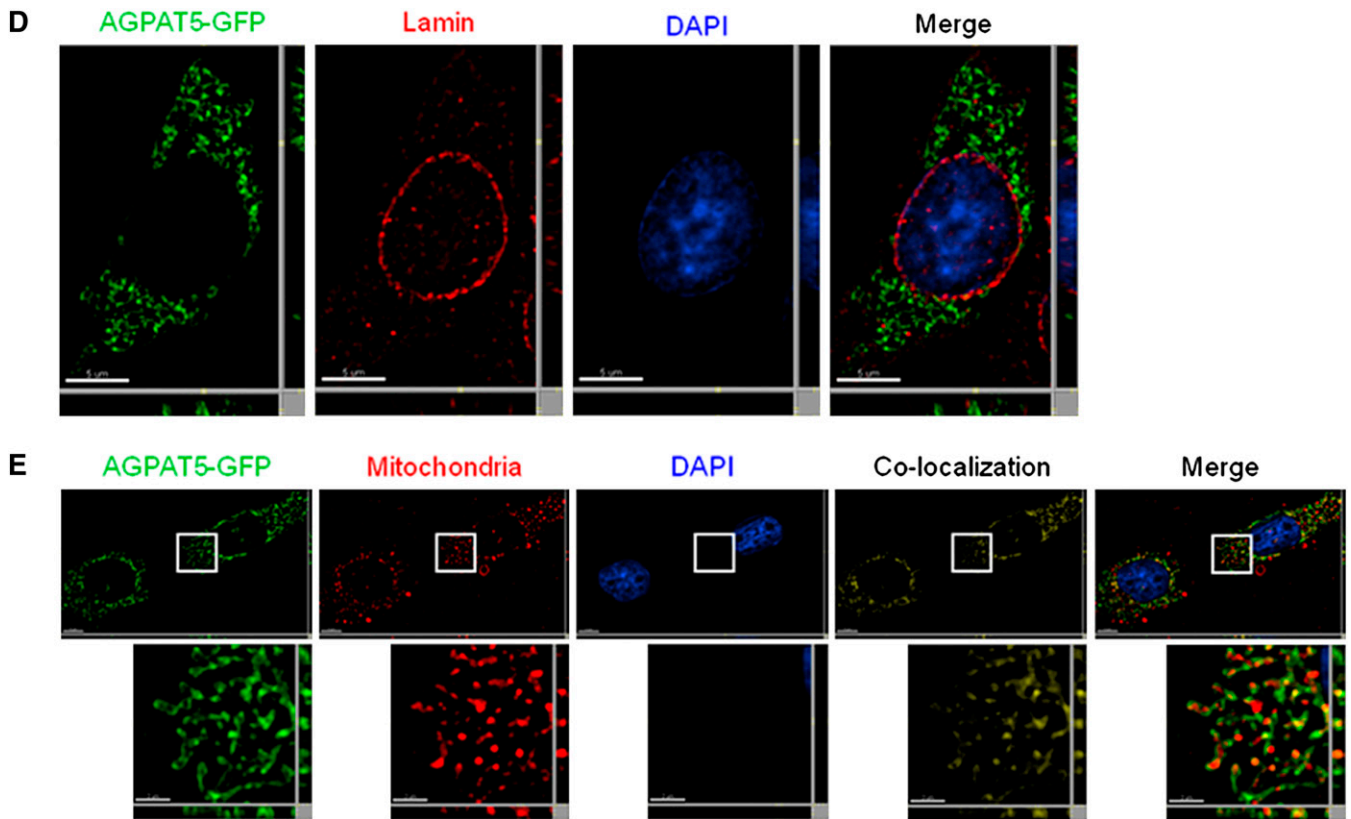
Fig. 1.—*Continued.*

(Invitrogen) for 2 h at room temperature. The membrane was washed and then incubated with ECL reagent (GE Healthcare, Piscataway, NJ) and exposed to X-ray film to visualize the immunoreactive protein. The same blots were stripped using Restore Western Blot Stripping Buffer (Thermo Scientific, Rockford, IL) according to the manufacturer's protocol, reprobed with anti-GAPDH antibody at a dilution of 1:5000, and detected with IgG conjugated with horseradish peroxidase at a dilution of 1:5000.

The mitochondrial and microsomal subcellular fractions (30 μg each) were resolved on a 4-15% gradient SDS-PAGE. The expression of AGPAT3 or AGPAT5 was detected with V5-antibody, whereas the presence of mitochondria or microsomes were detected with prohibitin (dilution 1:2500; Santa Cruz Biotechnologies, CA) or calnexin (dilution 1:2500; Santa Cruz Biotechnologies) specific for these subcellular fractions.

Immunofluorescence microscopy

CHO cells stably expressing AGPAT3-EGFP and AGPAT5-EGFP were grown on cover slips a day before the experiment. HeLa cells were plated on the cover slips in a 6-well plate and transiently transfected with 1.5 μg of AGPAT5-EGFP 24 h before the experiment. Cells were fixed and permeabilized by incubating them with methanol ($-20°C$) for 20 min. Cells were washed three times for 5 min with PBS and then incubated with primary antibody [(Sec61β at a dilution of 1:200 (Upstate, Lake Placid, NY) or lamin A/C at a dilution of 1:100 (Santa Cruz, CA)] for 60 min at 37°C in a humidified chamber. Cells were then washed three times for 5 min with PBS and incubated with AlexaFluor 594 coupled fluorescent secondary antibody (Invitrogen, Carlsbad, CA) for 60 min at 37°C in a humidified chamber. After incubation, cells were washed three times for 5 min with PBS,

counterstained with 4′-6-diamidino-2-phenylindole (DAPI) during the washes, and mounted on a glass slide with Aqua Poly/Mount (Polysciences, Warrington, PA). Cells were observed with DeltaVision RT Deconvolution Microscope (Applied Precision, Issaquah, WA). For mitochondrial visualization, the cells were incubated with a mitochondrial-specific dye (MitoTracker Red Dye 580; Molecular Probe, Eugene, OR) for 30 min in the incubation chamber, washed, fixed in 4% paraformaldehyde, washed, counterstained with DAPI, and mounted for microscopy.

Immunofluorescent cells were imaged with a Deltavision workstation (Applied Precision, Issaquah, WA). Z-stack images for green, red, and blue fluorescence were acquired in 0.15 micron steps at 60× magnification and were deconvolved using SoftWoRx (Applied Precision). Colocalization analysis was carried out using Imaris software (Bitplane, Zurich). The red and green channels were background subtracted using a rolling ball algorithm with the radius set to 0.5 μm. Systematic channel mis-registration was calculated from images of Tetraspeck beads (Invitrogen) taken under the same imaging conditions and corrected by shifting the red image -1, $+1$ and -1 in the x, y, and z directions, respectively. Maximum intensity projections for each channel are shown in the figures.

Quantitative real-time PCR in human tissue panel

Quantitative PCR was performed on a human cDNA panel from Clontech (Palo Alto, CA) using TaqMan primer and probes designed using PRIMER EXPRESS analysis software and analyzed using the ABI PRISM 7700 Sequence Detection System. To amplify AGPAT3, 100 pg of cDNA was added to the forward (5′-CTCCA-AGGTCCTCGCTAAGAAG-3′) and reverse (5′-CCGCTTGCAG-AACACAATCTC-3′) primers along with fam-labeled probe (GACCTGCACCATGAAA) and universal mix containing AmpliTaq and appropriate buffers. Similarly, AGPAT4 was amplified using primer forward (5′-CACGGAATGCACCATCTTCA-3′) and

reverse (5′-GAACCACGATGGCATTTTCCT-3′) primers along with fam-labeled probe (CGCCTACCTCAAGTAT). The PCR was followed for 40 cycles of 94°C for 15 s and 60°C for 30 s. The cDNA was amplified in duplicate along with *G3PDH* as an internal control. The ΔCt value for each tissue was calculated as ΔCt = [Ct (tissue) − Ct (G3PDH)] where necessary.

Statistical analysis

All quantitative enzymatic data are shown as mean ± SD. The *P* values were obtained using Student's *t*-test. Statistical analyses were performed using SigmaStat software.

RESULTS

Tissue distribution and quantitative expression in human tissue panel

The quantitative expressions of AGPAT3 and AGPAT4 in human tissues are shown in **Table 1**. AGPAT3 appears to be ubiquitously expressed across the tissues we examined. Among these tissues, the highest expression was detected in the testis, pancreas, and kidney, with slightly decreased expression in the spleen, lung, adipose tissue, and liver. The multiple protein alignment of known AGPATs reveals that human AGPAT3 is very close to human AGPAT4 (supplementary Fig. II). Quantitative real-time PCR revealed that the AGPAT4 isoform is also expressed in almost all of the tissues examined. In some tissues, such as the brain, ovary, and small intestine, AGPAT4 and AGPAT3 were expressed at similar levels, but in some tis-sues, like the kidney, liver, and skeletal muscle, the difference was more than 40-fold between the two isoforms. We had previously reported the expression of human AGPAT5 (10) and have included it here for comparison. It is interesting to note that the expression pattern of AGPAT4 and AGPAT5 are very similar, except for the leukocyte.

Subcellular localization of AGPAT3-GFP and AGPAT5-GFP

In CHO cells stably expressing the human AGPAT3-GFP fusion protein, fluorescence microscopy showed an endoplasmic reticulum (ER)-like expression pattern. This subcellular localization was confirmed by colocalizing AGPAT3-GFP with the ER-specific protein sec61-β (**Fig. 1A**). Intense staining was also observed when the cells were probed with the antibodies specific for lamin A/C, which is specific for nuclear lamina expression, indicating its presence in the nuclear envelope as well (Fig. 1B). AGPAT5-GFP fusion protein was also detected in the ER and the nuclear envelope (Fig. 1C, D). We also observed its presence in the mitochondria (Fig. 1E). The mitochondrial subcellular localization for AGPAT5-GFP was further confirmed in HeLa cells, except that the cells were transiently transfected with the AGPAT5-GFP construct. Here again, AGPAT5-GFP was localized to mitochondria (supplementary Fig. III). Lack of specific antibody to the AGPAT5 protein precluded us from demonstrating the presence of AGPAT5 protein in the mitochondria in its native state (supplementary Fig. IV). Computational analysis also
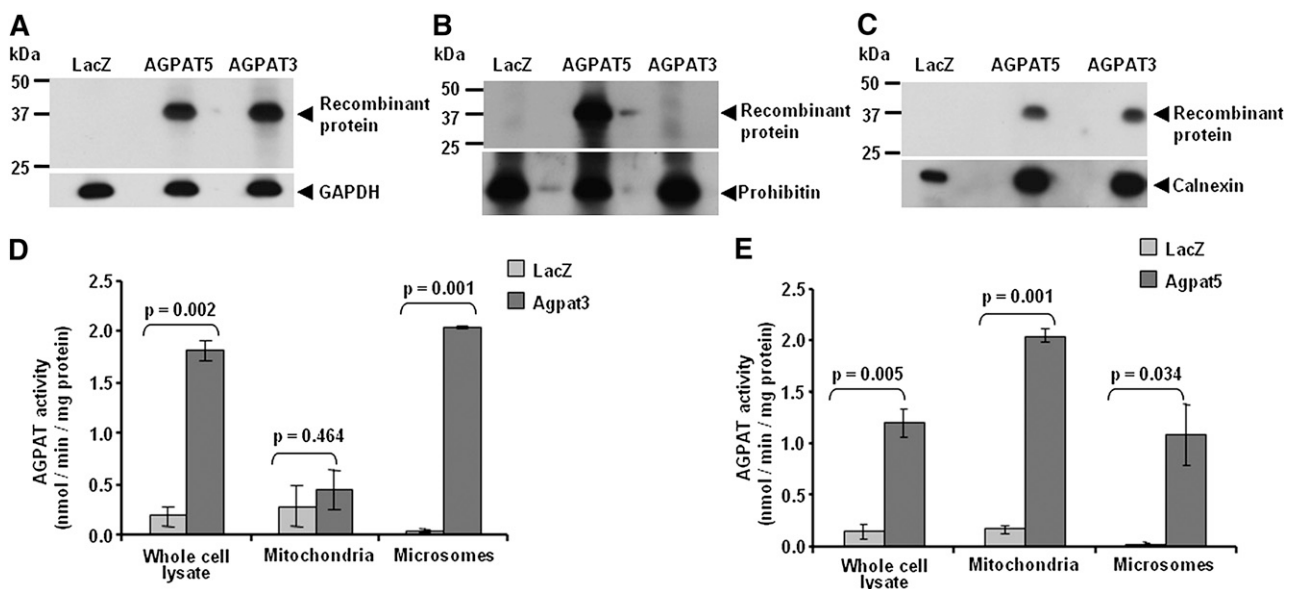

Fig. 2. Enzymatic activity and Western blot of wild-type human V5-AGPAT3 and V5-AGPAT5 expressed in AD293 cells. A: The Western blot for the recombinant AGPAT3 and AGPAT5 proteins from the whole-cell lysate as probed with V5-antibody. Lysates from cells infected with LacZ were loaded as a negative control. The same blot was stripped and reprobed with full form GAPDH to demonstrate protein loading. B: The Western blot shows the presence of AGPAT5 but absence of AGPAT3 in the mitochondrial fraction. The blot was also probed for the mitochondria-specific protein prohibitin. C: The Western blot for the presence of AGPAT3 and AGPAT5 in the microsomal fraction of the cell. The blot was also reprobed with calnexin, specific for the microsomes. D: The AGPAT activity in whole-cell lysate for AGPAT3 as determined by conversion of ^{3}H-LPA to ^{3}H-PA in the presence of oleoyl-CoA and expressed as product (^{3}H-PA) formed nmol per min per mg protein. The LPA to PA conversion by recombinant β-galactosidase adenovirus was used as a control. E: The enzymatic activity for AGPAT5. Not shown is the conversion of substrate in the absence of enzyme. Each bar represents mean ± SD from two independent experiments carried out in triplicate. The *P* value is shown above the bars. AGPAT, 1-acylglycerol-3-phosphate-O-acyltransferase; LacZ, recombinant adenovirus β-galactosidase.

revealed that human AGPAT5 had a probability of 0.95 to be localized to the mitochondria, whereas human AGPAT3 had the probability of only 0.82 (32).

Comparison of AGPAT3 and AGPAT4

Alignment of human *AGPAT1* through five amino acid sequences revealed that *AGPAT3* was more similar to *AGPAT4* than to any other acyltransferases (AGPAT1, 2, or 5) shown in supplementary Fig. II (12). The two isoforms are 75.1% homologous or 61.4% identical at the amino acid level. The signature motifs involved in catalytic and substrate binding, NHX_4D and EGTR, are conserved in the phospholipid acyltransferases. However, alignment of human AGPAT5 isoform appears to be a singleton, having the conserved acyltransferase motifs but with considerable decrease in the overall homology. AGPAT5 is only about 38% homologous or 20% identical to AGPAT3 and AGPAT4.

AGPAT activity

To confirm the expression of recombinant AGPAT3 and AGPAT5 proteins, we initially used whole-cell lysates or mitochondria and microsome subcellular fractions that we subjected to Western blot analysis. As shown in **Fig. 2A**-C, the expression of AGPAT3 and AGPAT5 could be recovered in the whole-cell lysate and microsomes. The predicted molecular weight of the wild-type AGPAT3 and AGPAT5 proteins were 43.38 and 42.07 kDa, respectively. AGPAT5 was also observed in the mitochondria, whereas AGPAT3 was not localized to mitochondria. This observation is consistent with the immunofluorescence localization of AGPAT3-GFP and AGPAT5-GFP fusion protein in CHO cells. Thus, AGPAT5 enzymatic activity was recovered in whole-cell lysate as expected, but it was significantly enriched in the mitochondrial fraction as well as in the microsomal fraction, whereas AGPAT3 enzymatic activity was only recovered in the whole-cell lysate and microsomal

fraction (Fig. 2D, E). As AGPAT5, but not AGPAT3, was found in both mitochondrial and microsomal fractions, for all further enzymatic assays, we employed the postnuclear fraction.

Substrate specificity of AGPAT3 and AGPAT5

Because human AGPAT3 and AGPAT5 revealed AGPAT activity, we then determined their acyl-CoA and LPA specificities. We employed a panel of LPAs with various long-chain fatty acids at the *sn-1* position and used radiolabeled oleoyl-CoA and radiolabeled arachidonoyl-CoA to determine the AGPAT activity. AGPAT3 appears to have a broader preference for LPA containing saturated or unsaturated fatty acids C16:0-C20:4 (**Fig. 3A**). However, this preference for LPA is further increased when C20:4 is used as the acyl donor. As shown, when C20:4 is a fatty acid donor and there is an odd number carbon chain fatty acid at the *sn-1* position of the LPA, the enzymatic activity increases by about 50%. Such LPA or fatty acid specificities were not evident with AGPAT5 (Fig. 3B). Nevertheless, the specificity for LPA or fatty acids remains broad, as observed for AGPAT3 using two different acyl donors (C18:1 and C20:4). For each LPA species used in this study, we also determined the AGPAT activity of the cellular lysate obtained from LacZ-expressing cells (supplementary Fig. V). AGPAT3 and AGPAT5 show similar specificities for the panel of saturated fatty acids used in this study (C8:0-C26:0) (**Fig. 4A**, B). However, only long-chain saturated fatty acids were a preferred substrate. Medium- and very long-chain fatty acids failed to acylate the LPA. Among unsaturated fatty acids, C18:1 remains the most preferred fatty acid for both of the isoforms studied. However, there are few differences as well. AGPAT3 could use C18:2 or C20:4 in addition to C18:1, but at only half the rate of C18:1. Differences emerged for AGPAT5, which also prefers C18:1 but failed to use C18:2. From the fatty acid panel we used, it appears that C18:2 could be used to differenti-
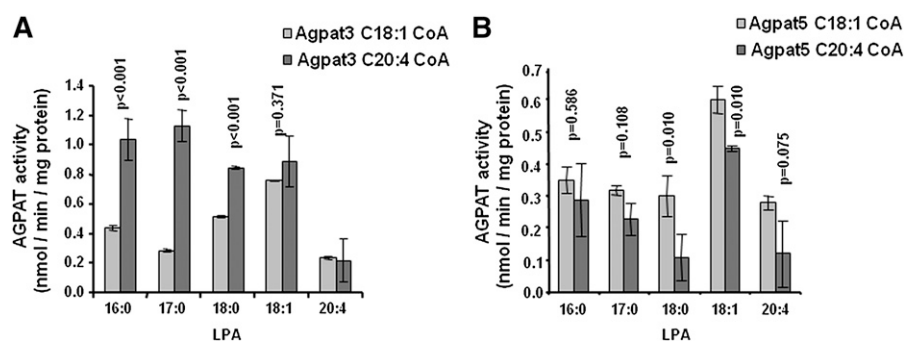

Fig. 3. Specificity of AGPAT3 and AGPAT5 for various LPAs. A: Shows LPA specificity of recombinant human AGPAT3 expressed in AD293 cells. Specificity of human recombinant AGPAT3 for various species of *sn-1*-lysophosphatidic acid acceptors was determined using radioactive oleoyl-CoA and arachidonoyl-CoA as donors. Activities are expressed as product (^{14}C-PA) formed nmol per min per mg protein. All enzymatic activities were determined in two independent experiments in triplicate. Bar represents mean ± SD. The *P* values are shown above the bars. B: Shows LPA specificity of recombinant human AGPAT5 expressed in AD293 cells. The LPA specificity of human recombinant AGPAT5 was determined and expressed as for AGPAT3. All enzymatic activities were determined in two independent experiments in triplicate. Each bar represents mean ± SD. The *P* values are shown above the bars. AGPAT, 1-acylglycerol-3-phosphate-O-acyltransferase; LPA, lysophosphatidic acid.
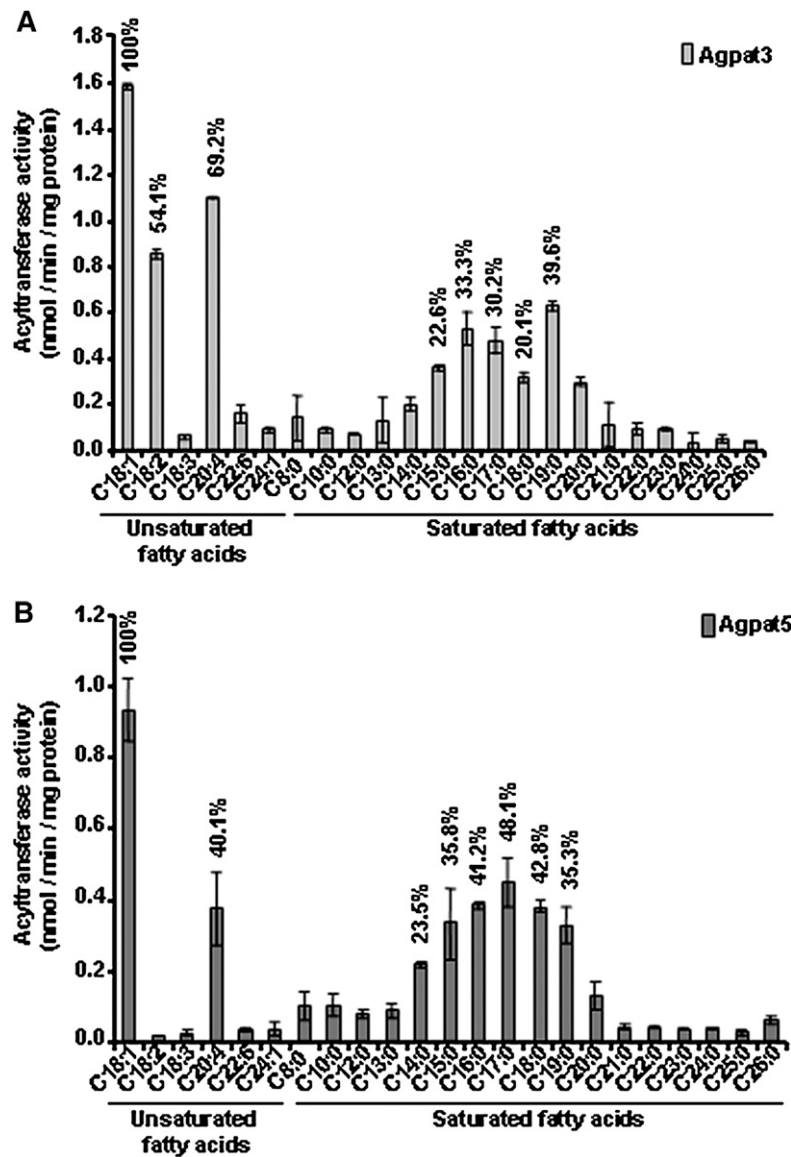
Fig. 4. Acyl-CoA specificity of recombinant human AGPAT3 and AGPAT5 expressed in AD293 cells. Specificity of human recombinant AGPAT3 (A) and AGPAT5 (B) for acyl-CoA donors was determined using *sn-1*-oleoyl-lysophosphatidic acid as an acceptor and various short-, medium-, and long-chain fatty acyl-CoA as donors. The enzymatic activity is compared with C18:1 (100%) (shown on top of the bar). Percent activity is marked only for those acyl CoA species which have least 20% of the activity compared with C18:1. All enzymatic activities were determined in two independent experiments in triplicate. Each bar represents mean ± SD. The *P* values are shown above the bars. AGPAT, 1-acylglycerol-3-phosphate-O-acyltransferase.

ate between the two isoforms, at least in in vitro studies. AGPAT activity with LacZ cellular lysates was also determined, but only for those acyl-CoAs that had demonstrable enzymatic activity (supplementary Fig. VI).

As most other AGPATs have other acyltransferase activities, we used LPS, LPE, LPI, LPC, and LPG to ascertain whether AGPAT3 and AGPAT5 could esterify these lysophospholipids (**Fig. 5A**, B). LPA is the most preferred lysophospholipid when either C18:1 or C20:4 fatty acids are used for the AGPAT3 isoform, while lysophospholipids LPC, LPI, and LPS also reveal appreciable enzymatic activity. For each lysophospholipid species used in this study, we also determined the LPLAT activity from the cellular lysate obtained from LacZ-expressing cells (supplementary Fig. VII). This study corroborates the previous study showing specificity for LPC and LPI by AGPAT3 (30). In this study, however, we show that LPS is also a substrate for AGPAT3. Contrarily, our study is at variance with the earlier study where C18:1 was not an effective substrate for AGPAT3 (30). We observed almost equal enzymatic activity with both the fatty acids C18:1 and C20:4. This difference in the enzymatic activity with these two acyl-CoAs may be due to the two different expression systems employed to study AGPAT3. The previous study (30) used a plasmid-based expression system, whereas the present study used a viral expression system. AGPAT5 has a similar, but not identical, pattern for the usage of various lysophospholipids used in this study. The most prominent effect was seen
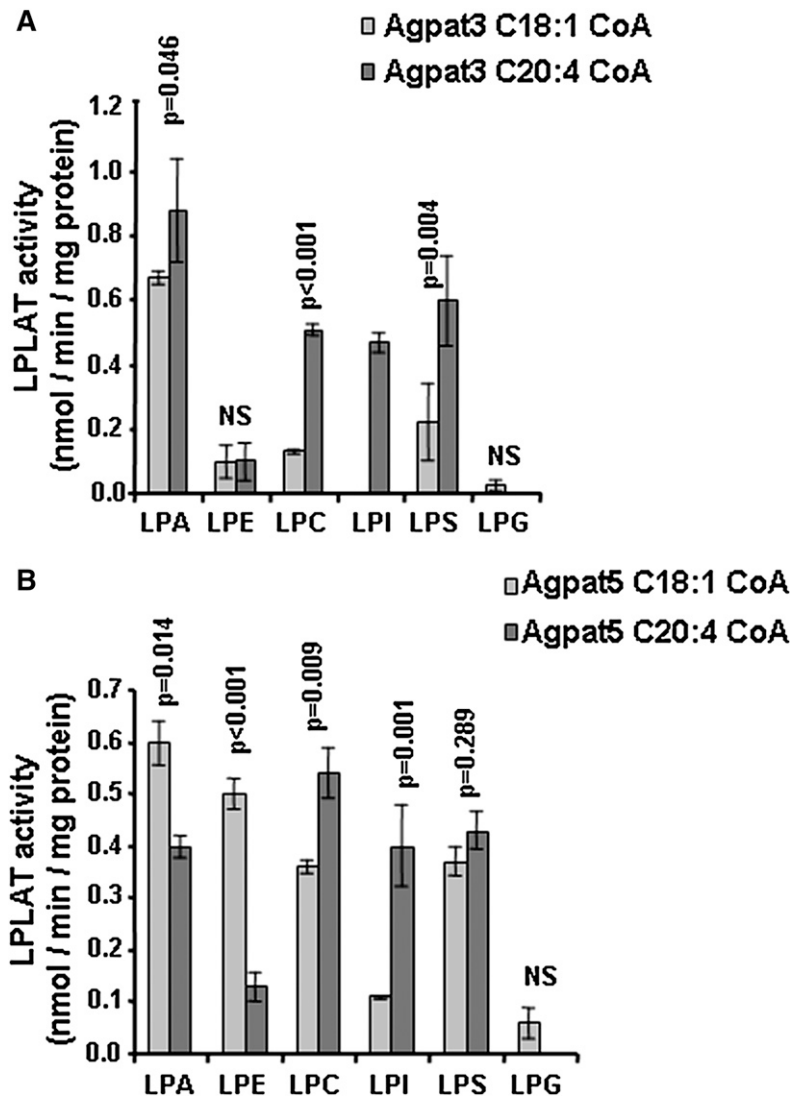
Fig. 5. Specificity for acyltransferase activity of AGPAT3 and AGPAT5 for lysophospholipids LPA, LPC, LPG, LPI, LPE, and LPS. A: The enzymatic activity for AGPAT3 was determined as the conversion of various lysophospholipids to their corresponding [14C]phospholipids in the presence of [14C] oleoyl-CoA or [14C]arachidonoyl-CoA and expressed as [14C]phospholipids product formed in nmol per min per mg protein. LacZ was used as a control. Shown are the mean values from two independent assays carried out in triplicate. Each bar represents mean ± SD. The *P* values are shown above the bars. B: The enzymatic activity of AGPAT5 for various lysophospholipids (determined as described for AGPAT3). Shown are the mean values from two independent assays carried out in triplicate. Each bar represents mean ± SD. The *P* values are shown above the bars. AGPAT, 1-acylglycerol-3-phosphate-O-acyltransferase; LacZ, recombinant adenovirus β-galactosidase; LPA, lysophosphatidic acid; LPE, lysophosphatidylethanolamine; LPI, lysophosphatidylinositol; LPC, lysophosphatidylcholine; LPS, lysophosphatidylserine; LPG, lysophosphatidylglycerol.

with LPE. A significant enzymatic activity was recovered for LPE with oleoyl-CoA, whereas arachidonoyl-CoA was inactive. This relationship was reversed with LPI, where arachidonoyl-CoA was active while oleoyl-CoA was not. LPG did not display any enzymatic activity with either fatty acid.

Enzyme kinetics

Knowing the preferred LPA and acyl-CoA for the enzyme AGPAT3 and AGPAT5, we then systematically determined the optimum temperature, pH, time of incu-

bation, and protein concentration (supplementary Figs. VIII and IX) to further undertake the kinetic studies. We determined the apparent rate of conversion (V_{max}) and Michaelis-Menten (K_m) constant for human AGPAT3 and AGPAT5 for both the acyl acceptor (LPA *sn-1* C18:1) and acyl donor (C18:1) (**Fig. 6A**-D). Surprisingly, the K_m for LPA for both of the isoforms remains almost the same (AGPAT3: 5.02; AGPAT5: 6.79), while the turnover of the enzyme AGPAT3 was three times faster than that of AGPAT5. A similar enzymatic kinetic pattern was observed when C18:1 was used as a substrate (**Table 2**).
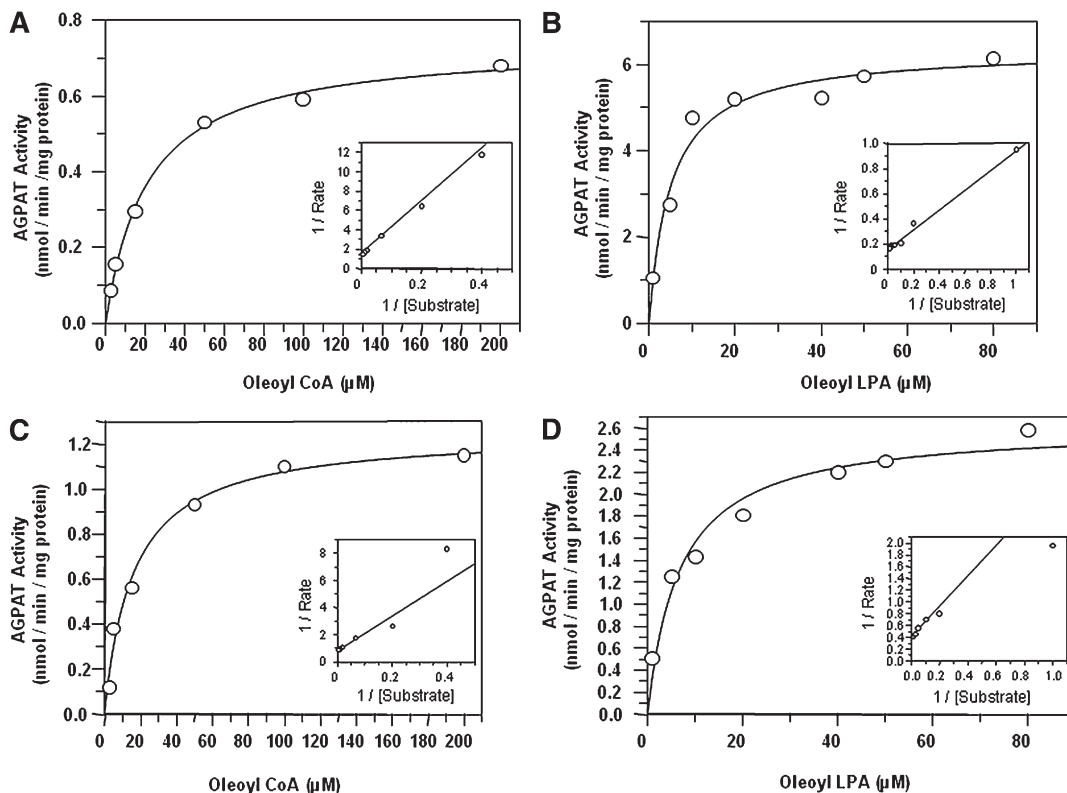
Fig. 6. Kinetic studies of recombinant human AGPAT3 and AGPAT5 expressed in AD-293 cells. A: The saturation curve of AGPAT3 enzymatic activity as determined by varying the concentration of oleoyl-LPA spiked with a known amount of [^{14}C]oleoyl-CoA. B: The saturation curve of AGPAT3 enzymatic activity as determined by incubating increasing concentrations of LPA with a fixed amount of [^{14}C]oleoyl-CoA. In A and B, the data were transformed to fit the Lineweaver-Burk plot to determine the K_m and V_{max} (shown as an insert). The enzymatic activities were determined in triplicate with each experiment carried out in triplicate. C: The saturation curve of AGPAT5 enzymatic activity as determined by varying the concentration of oleoyl-LPA spiked with a known amount of [^{14}C]oleoyl-CoA. D: The saturation curve of AGPAT3 enzymatic activity as determined by incubating increasing concentrations of LPA with a fixed amount of [^{14}C]oleoyl-CoA. In C and D, the enzymatic data were transformed as above to obtain the K_m and V_{max} (shown as an insert). Only representative graphs are shown. All experiments were performed in triplicate. The values were determined using GraFit software (Erithacus Software Ltd., Surrey, RH6 9YJ, UK). AGPAT, 1-acylglycerol-3-phosphate-O-acyltransferase; LPA, lysophosphatidic acid.

DISCUSSION

The presence of AGPAT5 in the mitochondria (this study) combined with the previous observations of GPAT1 and GPAT2 expression in mitochondria (33, 34) indicate that mitochondria are capable of synthesizing some of their own glycerophospholipids, at least in those tissues in which AGPAT5 is highly expressed or upregulated under various physiological conditions. In addition, as phospholipids greatly contribute toward the membrane curvature, it is possible that AGPAT5 has an important role in mitochondrial fusion and fission, although in this study we have not ruled out the contribution of other AGPAT isoforms that might be involved in this process. We demonstrate that the recombinant human AGPAT3 and AGPAT5 proteins localize to the ER and the nuclear envelope, a continuum of the ER, which might provide some of the phospholipids specifically suited for the nuclear function. Although not investigated in this study, mouse AGPAT3 is also localized in Golgi apparatus of the cell (29).

The highest tissue expression for human AGPAT5 was found in the testis. Since whole testis was used in the present study, it will be interesting to further determine in which testicular cell type AGPAT5 is expressed and when it is turned on during early development. We also noted that the AGPAT5 isoform is active in an acidic pH range from 7.4 to 5.5, which suggests it will remain enzymatically active when other AGPAT isoforms may be inactive. We can only speculate that this enzyme may have a role in sperm maturation (35).

The AGPAT3 isoform prefers LPA with oleic acid at its *sn-1* position as an acyl acceptor and oleoyl-CoA as the acyl donor. We show that AGPAT3 displays acyltransferase activity toward other lysophospholipids, such as LPC, LPS, and LPI, but only when arachidonic acid (C20:4) is used as an acyl donor. This will produce *sn-1*-C18:1; *sn-2*-C20:4 phosphatidic acid with a choline, serine, or inositol polar head. The reason why an unsaturated fatty acid is preferred by these lysophospholipids is unclear.

AGPAT5 has very similar substrate preference like AGPAT3. However, some differences were observed, such as AGPAT5 showing a clear preference for C18:1 over C20:4 for acylation of LPE. Thus, AGPAT5 will produce *sn-1*-C18:1; *sn-2*-C18:1-PE while remaining inactive toward C20:4.

TABLE 2. Mean apparent affinity (K_m) and maximum velocity (V_{max}) of human AGPAT3 and AGPAT5 (this study) and those of AGPAT10/GPAT3/AGPAT8 (NP_116106) and AGPAT2

Substrate	K_m (µM)	V_{max} (nmol/min/mg protein)	V_{max}/K_m
AGPAT 3			
Acyl CoA	21.53	0.74	0.04
LPA	4.78	6.35	1.33
AGPAT5			
Acyl CoA	16.30	1.22	0.08
LPA	5.52	2.42	0.44
AGPAT10/GPAT3/AGPAT8[a]			
Acyl-CoA	2.7	60	22
LPA	9.2	14.19	1.5
AGPAT2[b]			
Acyl-CoA	0.4	210	525
LPA	2	200	100

The human AGPAT3, AGPAT5 and AGPAT10/GPAT3/AGPAT8 were expressed in AD-293 cells using recombinant adenovirus, whereas human AGPAT2 was expressed in Sf9 cells using recombinant baculovirus. Kinetic parameters for the proteins were determined using unpurified recombinant proteins. AGPAT, 1-acylglycerol-3-phosphate-O-acyltransferase; LPA, lysophosphatidic acid.
[a]Data from Ref. 12.
[b]Data from Ref. 36.

The enzyme kinetic studies show that AGPAT3 has an apparent affinity constant (K_m) of 5.02 µM at half maximal velocity with an apparent V_{max} of 6.35 nmol/min/mg protein for LPA. The apparent K_m and V_{max} was several-fold lower for acyl-CoA, being 20.99 µM and 0.034 nmol/min/mg protein, respectively (Table 2). The kinetic parameters for AGPAT5 were not very different from those of AGPAT3. The apparent K_m was 6.78 µM at half maximal velocity with an apparent V_{max} of 2.62 nmol/min/mg protein for LPA. The apparent K_m and V_{max} were lower for acyl-CoA, being 16.23 µM and 0.07 nmol/min/mg protein, respectively (Table 2). Although the preferred substrates for AGPAT3 and AGPAT5 remain similar to those reported for AGPAT2, the kinetic parameters of these enzymes are quite different (36). Using human recombinant AGPAT2 obtained from insect Sf9 cells, the apparent K_m and V_{max} for 1-oleoyl-CoA were 0.4 µM and 210 nmol/min/mg protein, respectively. The enzyme kinetics of AGPAT2 for the other substrate LPA was 2.0 µM (K_m) with the V_{max} of 200 nmol/min/mg protein (36). This finding indicates that AGPAT2 has several-fold higher apparent affinity for the same substrates (acyl-CoA and LPA) than AGPAT3, AGPAT5, and previously reported AGPAT10/GPAT3 (12). The catalytic activity is a measure of enzymatic activity in the cells. As shown in Table 2, AGPAT3 and AGPAT5 are at least 100-fold less efficient compared with human AGPAT2 enzyme (36). Although the vectors employed to obtain recombinant proteins are different, this and our previous studies indicate that AGPAT2 will be the preferred enzyme over AGPAT10/GPAT3, AGPAT3, and AGPAT5 for acylation in tissues where it is expressed more than the other isoforms, particularly in adipocytes. Thus the enzyme kinetic study suggests that these other isoforms may be involved mostly in providing various phospholipids for maintaining membrane structure and function rather than TAG synthesis.

Human *AGPAT3* is located on chromosome 21 (nt: 45,285,067-45,406,417) and consists of nine exons, where exon 1 is untranslated (supplementary Table III). Human *AGPAT5* is localized on chromosome 8 (nt: 6565878-6619019) and consists of eight exons (supplementary Table IV). Human *AGPAT3* is highly conserved among the chimpanzee, chicken, *D. melanogaster, A. thaliana,* mouse, and *zebrafish. AGPAT5* is also conserved in all the species except *A. thaliana.* Tissue expression patterns, using quantitative RT-PCR analysis, revealed that AGPAT3 is highly expressed in the lung, spleen, and leukocytes, and it is also present in most other tissues. It is least expressed in the heart, liver, and thymus.

PA and diacylglycerol, a dephosphorylated product of PA, are precursors for the biosynthesis of various phospholipids and TAG. It is possible that all enzymatic activity for the AGPAT enzymes is within the membrane where they are localized. The phospholipids are integral components of all the cellular membranes, including those of mitochondria, ER, peroxisomes, and plasma membrane. For ER and mitochondrial biogenesis there is local demand for specific phospholipid species. AGPAT isoforms might fulfill this location specific role. Future experiments will be directed toward understanding the specific role of each of these AGPATs in tissue models to determine specific subcellular localization (micro domain). To understand these functions, an antibody to each of the AGPAT isoforms is required to confirm subcellular localization identified with our GFP-fusion proteins. Determining the role of these enzymes will be benefitted immensely by generating mouse models by homologous gene deletion to understand their function in whole animals. In this context, it is important to mention that when *Agpat2* null mice were generated and analyzed, an unexpected role of monoacylglycerol acyltransferase 1 in the biosynthesis of TAG in liver was discovered (15).

Our goal has been to identify new isoforms for the AGPAT enzymes and characterize their tissue expression patterns and enzymatic activities in the hope that one of these isoforms, in addition to AGPAT2, is highly expressed in the adipose tissue, which might provide additional genetic loci for patients with lipodystrophy. Based on the expression and enzymatic kinetic data for AGPAT3 and AGPAT5, their role in the synthesis of TAG may be minimal at best. However, this study also revealed that among the AGPAT isoforms studied thus far, only AGPAT5 when overexpressed localizes to the mitochondria. The confirmation of AGPAT5 localization to mitochondria awaits the generation of suitable antibody to the AGPAT5 protein. Its possible function in mitochondrial physiology remains to be elucidated.

REFERENCES

1. Merkl, I., and W. E. Lands. 1963. Metabolism of glycerolipids. IV. Synthesis of phosphatidylethanolamine. *J. Biol. Chem.* **238:** 905–906.

2. Agarwal, A. K., and A. Garg. 2003. Congenital generalized lipodystrophy: significance of triglyceride biosynthetic pathways. *Trends Endocrinol. Metab.* **14:** 214–221.

3. Coleman, R. A., and D. P. Lee. 2004. Enzymes of triacylglycerol synthesis and their regulation. *Prog. Lipid Res.* **43:** 134–176.

4. Takeuchi, K., and K. Reue. 2009. Biochemistry, physiology, and genetics of GPAT, AGPAT, and lipin enzymes in triglyceride synthesis. *Am. J. Physiol. Endocrinol. Metab.* **296:** E1195–E1209.

5. Eberhardt, C., P. W. Gray, and L. W. Tjoelker. 1997. Human lysophosphatidic acid acyltransferase. cDNA cloning, expression, and localization to chromosome 9q34.3. *J. Biol. Chem.* **272:** 20299–20305.

6. Leung, D. W. 2001. The structure and functions of human lysophosphatidic acid acyltransferases. *Front. Biosci.* **6:** d944–d953.

7. Aguado, B., and R. D. Campbell. 1998. Characterization of a human lysophosphatidic acid acyltransferase that is encoded by a gene located in the class III region of the human major histocompatibility complex. *J. Biol. Chem.* **273:** 4096–4105.

8. Beigneux, A. P., L. Vergnes, X. Qiao, S. Quatela, R. Davis, S. M. Watkins, R. A. Coleman, R. L. Walzem, M. Philips, K. Reue, et al. 2006. Agpat6-a novel lipid biosynthetic gene required for triacylglycerol production in mammary epithelium. *J. Lipid Res.* **47:** 734–744.

9. Ye, G. M., C. Chen, S. Huang, D. D. Han, J. H. Guo, B. Wan, and L. Yu. 2005. Cloning and characterization a novel human 1-acyl-sn-glycerol-3-phosphate acyltransferase gene AGPAT7. *DNA Seq.* **16:** 386–390.

10. Agarwal, A. K., R. I. Barnes, and A. Garg. 2006. Functional characterization of human 1-acylglycerol-3-phosphate acyltransferase isoform 8: cloning, tissue distribution, gene structure and enzymatic activity. *Arch. Biochem. Biophys.* **449:** 64–76.

11. Agarwal, A. K., S. Sukumaran, R. Bartz, R. I. Barnes, and A. Garg. 2007. Functional characterization of human 1-acylglycerol-3-phosphate-O-acyltransferase isoform 9: cloning, tissue distribution, gene structure, and enzymatic activity. *J. Endocrinol.* **193:** 445–457.

12. Sukumaran, S., R. I. Barnes, A. Garg, and A. K. Agarwal. 2009. Functional characterization of the human 1-acylglycerol-3-phosphate-O-acyltransferase isoform 10/glycerol-3-phosphate acyltransferase isoform 3. *J. Mol. Endocrinol.* **42:** 469–478.

13. Agarwal, A. K., and A. Garg. 2010. Enzymatic activity of the human 1-acylglycerol-3-phosphate-O-acyltransferase isoform 11: upregulated in breast and cervical cancers. *J. Lipid Res.* **51:** 2143–2152.

14. Agarwal, A. K., E. Arioglu, S. de Almeida, N. Akkoc, S. I. Taylor, A. M. Bowcock, R. I. Barnes, and A. Garg. 2002. *AGPAT2* is mutated in congenital generalized lipodystrophy linked to chromosome 9q34. *Nat. Genet.* **31:** 21–23.

15. Cortes, V. A., D. E. Curtis, S. Sukumaran, X. Shao, V. Parameswara, S. Rashid, A. R. Smith, J. Ren, V. Esser, R. E. Hammer, et al. 2009. Molecular mechanisms of hepatic steatosis and insulin resistance in the AGPAT2-deficient mouse model of congenital generalized lipodystrophy. *Cell Metab.* **9:** 165–176.

16. Radner, F. P., I. E. Streith, G. Schoiswohl, M. Schweiger, M. Kumari, T. O. Eichmann, G. Rechberger, H. C. Koefeler, S. Eder, S. Schauer, et al. 2010. Growth retardation, impaired triacylglycerol catabolism, hepatic steatosis, and lethal skin barrier defect in mice lacking comparative gene identification-58 (CGI-58). *J. Biol. Chem.* **285:** 7300–7311.

17. Lewin, T. M., P. Wang, and R. A. Coleman. 1999. Analysis of amino acid motifs diagnostic for the sn-glycerol-3-phosphate acyltransferase reaction. *Biochemistry.* **38:** 5764–5771.

18. Schweiger, M., A. Lass, R. Zimmermann, T. O. Eichmann, and R. Zechner. 2009. Neutral lipid storage disease: genetic disorders caused by mutations in adipose triglyceride lipase/PNPLA2 or CGI-58/ABHD5. *Am. J. Physiol. Endocrinol. Metab.* **297:** E289–E296.

19. Vergnes, L., A. P. Beigneux, R. Davis, S. M. Watkins, S. G. Young, and K. Reue. 2006. Agpat6 deficiency causes subdermal lipodystrophy and resistance to obesity. *J. Lipid Res.* **47:** 745–754.

20. Chen, Y. Q., M. S. Kuo, S. Li, H. H. Bui, D. A. Peake, P. E. Sanders, S. J. Thibodeaux, S. Chu, Y. W. Qian, Y. Zhao, et al. 2008. AGPAT6 is a novel microsomal glycerol-3-phosphate acyltransferase. *J. Biol. Chem.* **283:** 10048–10057.

21. Nagle, C. A., L. Vergnes, H. Dejong, S. Wang, T. M. Lewin, K. Reue, and R. A. Coleman. 2008. Identification of a novel sn-glycerol-3-phosphate acyltransferase isoform, GPAT4, as the enzyme deficient in Agpat6$^{-/-}$ mice. *J. Lipid Res.* **49:** 823–831.

22. Rajakumari, S., and G. Daum. 2010. Janus-faced enzymes yeast Tgl3p and Tgl5p catalyze lipase and acyltransferase reactions. *Mol. Biol. Cell.* **21:** 501–510.

23. Cao, J., Y. Liu, J. Lockwood, P. Burn, and Y. Shi. 2004. A novel cardiolipin-remodeling pathway revealed by a gene encoding an endoplasmic reticulum-associated acyl-CoA:lysocardiolipin acyltransferase (ALCAT1) in mouse. *J. Biol. Chem.* **279:** 31727–31734.

24. Chen, X., B. A. Hyatt, M. L. Mucenski, R. J. Mason, and J. M. Shannon. 2006. Identification and characterization of a lysophosphatidylcholine acyltransferase in alveolar type II cells. *Proc. Natl. Acad. Sci. USA.* **103:** 11724–11729.

25. Nakanishi, H., H. Shindou, D. Hishikawa, T. Harayama, R. Ogasawara, A. Suwabe, R. Taguchi, and T. Shimizu. 2006. Cloning and characterization of mouse lung-type acyl-CoA:lysophosphatidylcholine acyltransferase 1 (LPCAT1). Expression in alveolar type II cells and possible involvement in surfactant production. *J. Biol. Chem.* **281:** 20140–20147.

26. Cao, J., J. L. Li, D. Li, J. F. Tobin, and R. E. Gimeno. 2006. Molecular identification of microsomal acyl-CoA:glycerol-3-phosphate acyltransferase, a key enzyme in de novo triacylglycerol synthesis. *Proc. Natl. Acad. Sci. USA.* **103:** 19695–19700.

27. Shindou, H., D. Hishikawa, H. Nakanishi, T. Harayama, S. Ishii, R. Taguchi, and T. Shimizu. 2007. A single enzyme catalyzes both platelet-activating factor production and membrane biogenesis of inflammatory cells. Cloning and characterization of acetyl-CoA:LYSO-PAF acetyltransferase. *J. Biol. Chem.* **282:** 6532–6539.

28. Harayama, T., H. Shindou, R. Ogasawara, A. Suwabe, and T. Shimizu. 2008. Identification of a novel noninflammatory biosynthetic pathway of platelet-activating factor. *J. Biol. Chem.* **283:** 11097–11106.

29. Schmidt, J. A., and W. J. Brown. 2009. Lysophosphatidic acid acyltransferase 3 regulates Golgi complex structure and function. *J. Cell Biol.* **186:** 211–218.

30. Yuki, K., H. Shindou, D. Hishikawa, and T. Shimizu. 2009. Characterization of mouse lysophosphatidic acid acyltransferase 3: an enzyme with dual functions in the testis. *J. Lipid Res.* **50:** 860–869.

31. Haque, W., A. Garg, and A. K. Agarwal. 2005. Enzymatic activity of naturally occurring 1-acylglycerol-3-phosphate-O-acyltransferase 2 mutants associated with congenital generalized lipodystrophy. *Biochem. Biophys. Res. Commun.* **327:** 446–453.

32. Claros, M. G., and P. Vincens. 1996. Computational method to predict mitochondrially imported proteins and their targeting sequences. *Eur. J. Biochem.* **241:** 779–786.

33. Yet, S. F., S. Lee, Y. T. Hahm, and H. S. Sul. 1993. Expression and identification of p90 as the murine mitochondrial glycerol-3-phosphate acyltransferase. *Biochemistry.* **32:** 9486–9491.

34. Lewin, T. M., N. M. Schwerbrock, D. P. Lee, and R. A. Coleman. 2004. Identification of a new glycerol-3-phosphate acyltransferase isoenzyme, mtGPAT2, in mitochondria. *J. Biol. Chem.* **279:** 13488–13495.

35. Lishko, P. V., I. L. Botchkina, A. Fedorenko, and Y. Kirichok. 2010. Acid extrusion from human spermatozoa is mediated by flagellar voltage-gated proton channel. *Cell.* **140:** 327–337.

36. Hollenback, D., L. Bonham, L. Law, E. Rossnagle, L. Romero, H. Carew, C. K. Tompkins, D. W. Leung, J. W. Singer, and T. White. 2006. Substrate specificity of lysophosphatidic acid acyltransferase beta-evidence from membrane and whole cell assays. *J. Lipid Res.* **47:** 593–604.

37. Livak, K. J. 1997. ABI Prism 7700 Sequence Detection System. User Bulletin No. 2. *PE Applied Biosystems.* 11–15.